ELECTRONIC SUPPORTING INFORMATION

Ultrafast two-dimensional infrared spectroscopy resolves the conformational change of an Evans auxiliary induced by $Mg(ClO_4)_2$

Andreas T. Messmer, [§] Sabrina Steinwand, [§] Katharina M. Lippert,[‡] Peter R. Schreiner*[,‡] and Jens Bredenbeck*[,§,#]

[§] Institute of Biophysics; Johann Wolfgang von Goethe-University; Max-von-Laue-Str. 1; 60438 Frankfurt; Germany
[‡] Institute of Organic Chemistry, Justus-Liebig University; Heinrich-Buff-Ring 58; 35392 Giessen; Germany
[#] CEF-MC; Johann Wolfgang von Goethe-University; Max-von-Laue-Str. 9; 60438 Frankfurt; Germany

CONTENT

1 NORMAL MODE FREQUENCIES

Table S1 shows a comparison of the experimentally determined wavenumbers of bands ν_1, ν_2 and ν_3 of the main complex and the computed values for various **1**·Mg^{2+} complexes that have been discussed. For the chosen level of theory (M06/6–31+G(*d*,*p*)/PCM/Bondi), no wavenumber scaling factors have been established in the literature. For **1-spc-**κ^2*O,O'* however, agreement between computed and experimental values is best as the difference between the two is very similar for ν_1, ν_2 and ν_3 (Δ = 50 cm^{-1}, 57 cm^{-1} and 48 cm^{-1}), amounting to a uniform scaling factor of 0.97, or alternatively, a shift of –51 cm^{-1}. For the other structures the shift varies strongly between the different modes. For free **1**, an average shift of –47 cm^{-1} is found.[3]

Table S1. Comparison of the experimental vibrational wavenumbers and the computed (M06/6–31+G(*d*,*p*)/PCM/Bondi) values of various **1**·Mg^{2+} complexes in MeCN. The data for free **1** are shown in the last two columns.

		1·magnesium complexes					Free **1**[3]	
		experiment			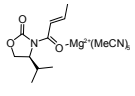	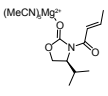	experiment	
		major species	**1-spc-** κ^2*O,O'*	**1-spt-** κ^2*O,O'*	**1-apc-** κ*O'*	**1-apc-** κ*O*		**1-apc**
wavenumber	ν_1 (cm^{-1})	1616	1665 (Δ=50)	1679 (Δ=63)	1673 (Δ=57)	1690 (Δ=74)	1639	1690 (Δ=51)
	ν_2 (cm^{-1})	1650	1707 (Δ=57)	1715 (Δ=65)	1719 (Δ=69)	1744 (Δ=94)	1687	1734 (Δ=47)
	ν_3 (cm^{-1})	1762	1810 (Δ=48)	1806 (Δ=44)	1836 (Δ=74)	1807 (Δ=45)	1776	1820 (Δ=44)

2 P2D-IR SPECTRA

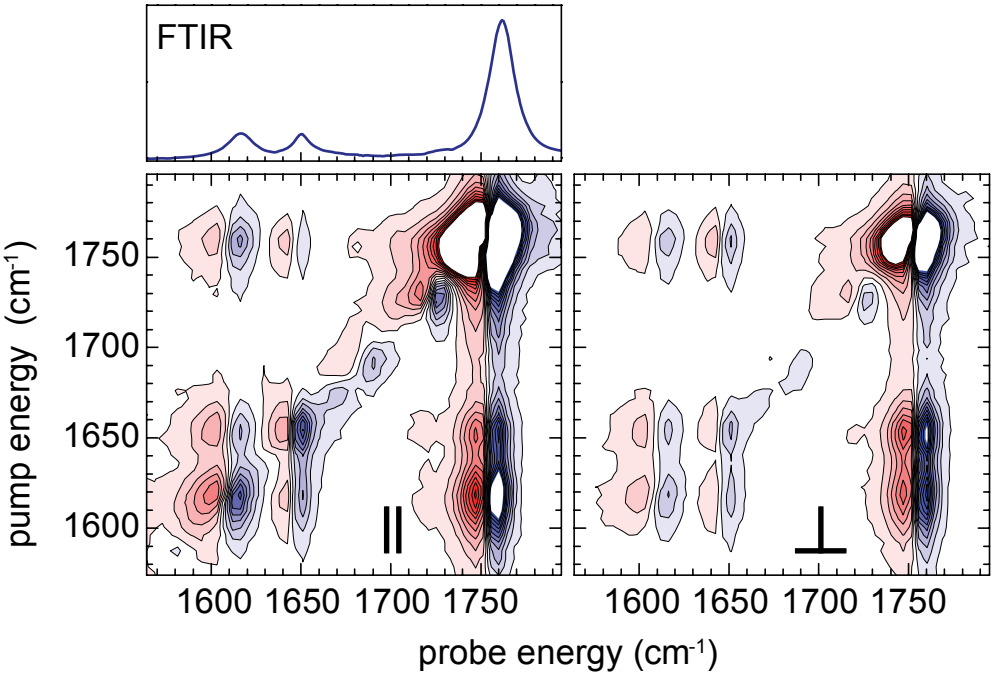

Figure S1. P2D-IR spectra (1.5 ps) of a solution of **1** (34 mM) and $Mg(ClO_4)_2$ (0.38 M) in MeCN for parallel (left) and perpendicular polarization (right). The contour lines are spaced by 0.05 mOD. Signals larger than ±0.5 mOD are truncated.

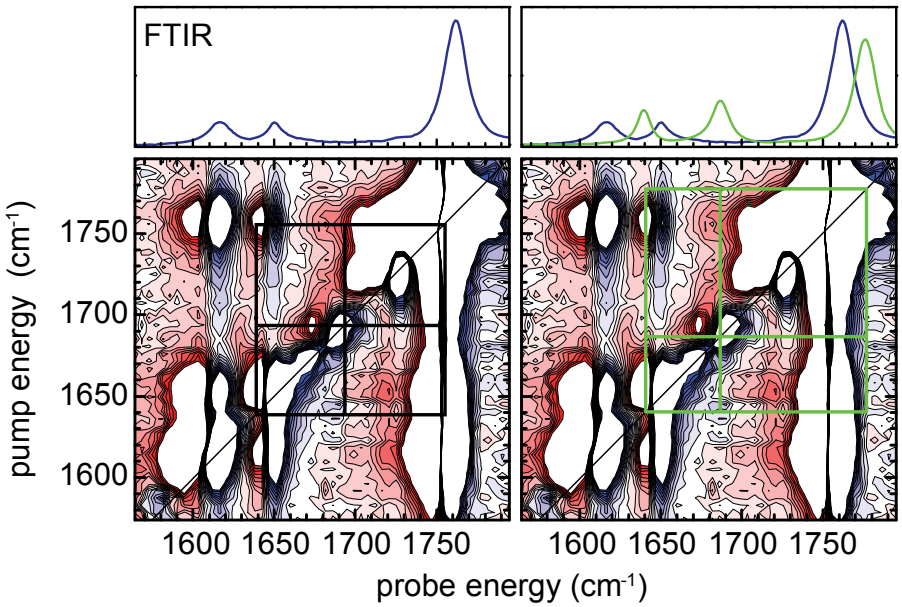

Figure S2. P2D-IR spectrum of **1** (34 mM) and $Mg(ClO_4)_2$ (0.38 M) in MeCN. (1.5 ps, parallel polarization). The contour lines are spaced by 6 µOD. Signals larger than ±0.06 mOD are truncated. The FTIR spectrum is shown in the top panel for orientation (blue: mixture of **1** and $Mg(ClO_4)_2$, green: free **1**). The grid for **1-apc-***κO*·$Mg^{2+}(MeCN)_5$ (black) is based on the DFT computation (see Table 1), while the grid for the coupling pattern for free **1** (green) is based on experimental data (*cf.* Fig. 2).

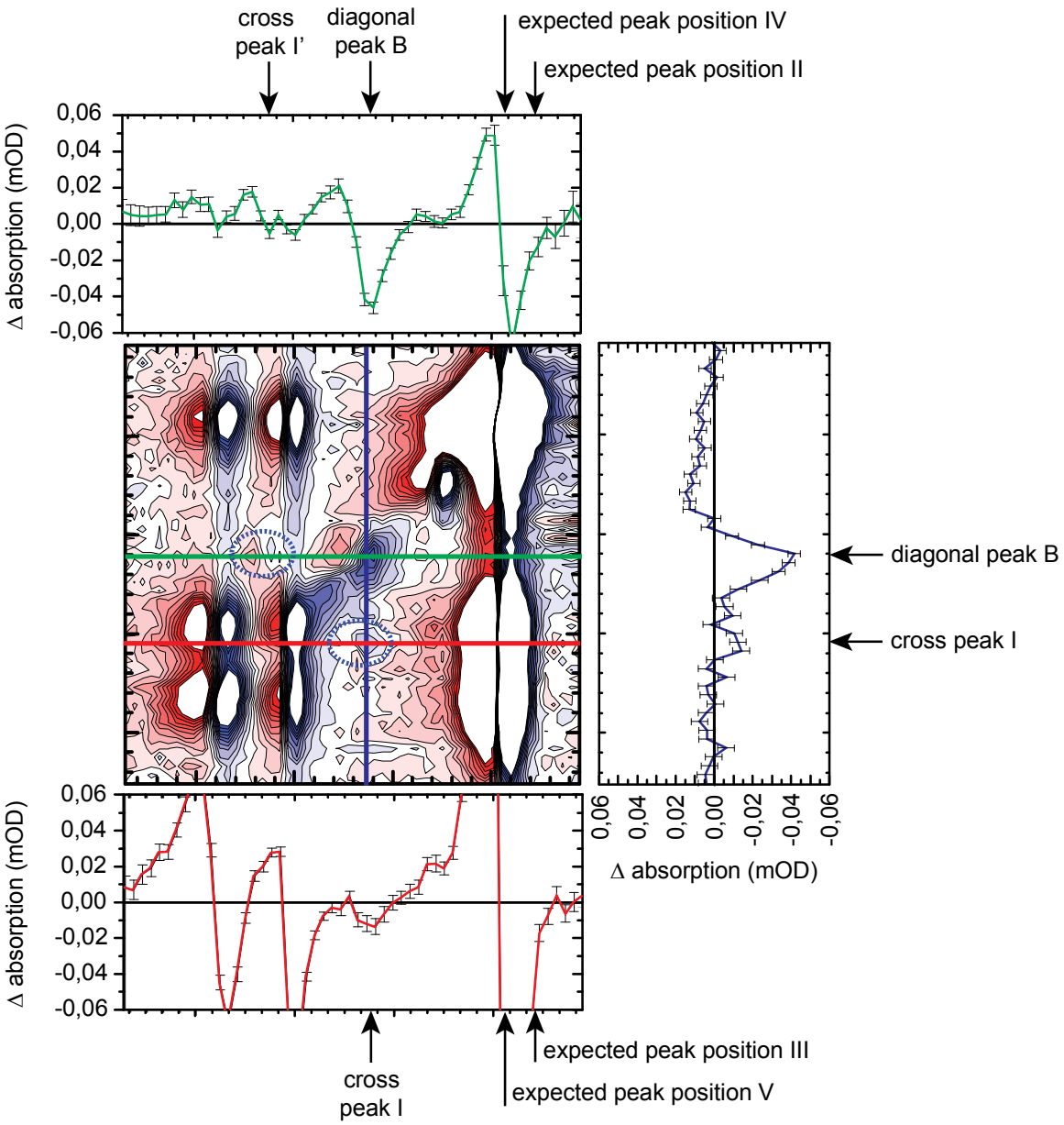

Figure S3. Figure 2 of the article is shown with cross sections of the spectrum. The position of each cross section (green, red and blue) in the 2D-IR spectrum is marked by a line in the according color. The expected positions of potential cross peaks II to IV in Figure 2 are marked by arrows in the cross sections. The arrows point to the expected position of the blue part (fundamental frequency) of the peak. Due to overlap with the strong signal of the main species, cross peaks at these positions cannot be observed. Cross peak I and its counterpart I´ can be seen in the cross sections.

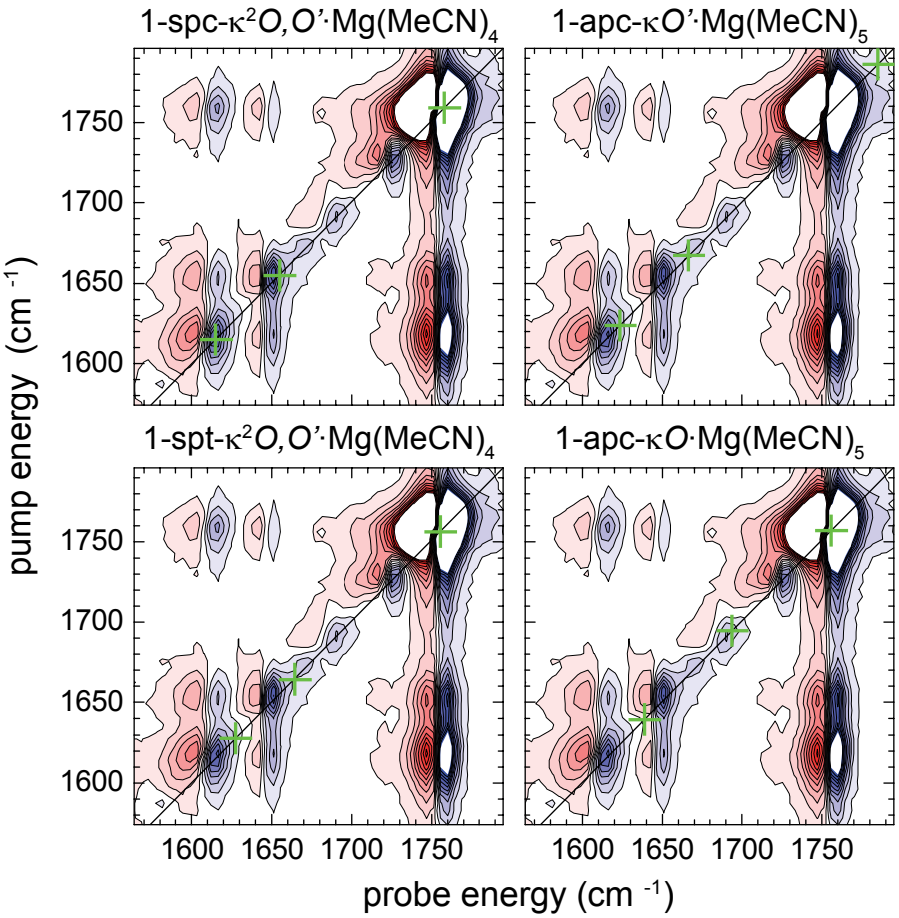

Figure S4. Computed positions (green crosses) of the diagonal peaks of the different Mg^{2+} complexes in the P2D-IR spectrum. All computed vibrational energies are corrected by –51 cm^{-1}.

3 ALTERNATIVE ANISOTROPY FIT

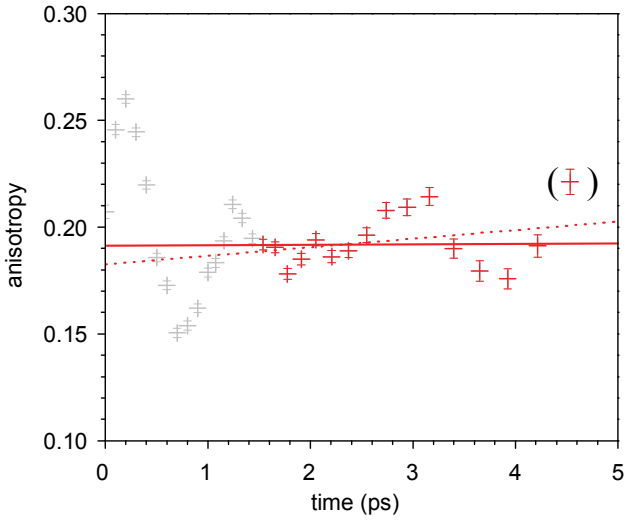

Figure S5. Anisotropy fit of the cross peak ν_1/ν_2 with (dashed line) and without the last data point (straight line) shown in brackets. The angles given by the two fits differ by only 1°.

Figure S5 compares the fit of the measured anisotropy of the cross peak ν_1/ν_2 with and without the last data point. The fit without the last data point shown in brackets (straight line) extrapolated to an anisotropy of $r(0\ \text{ps}) = 0.191(10)$, corresponding to an angle of 36°. The fit with all shown red data points led to an anisotropy of $r(0\ \text{ps}) = 0.183(2)$. This translates into an angle between the transition dipole moments of 37°. The two angles differ only by 1°, which is less than our experimental error. However, the dashed fit shows an increase of the anisotropy with longer delay time. Such a long term rise in anisotropy is physically not reasonable. The positive slope of the fit is caused by an oscillation on the anisotropy, which could be due to a coherent effect, since the two involved vibrations are close in energy. Similar effects have been observed for rhodium dicarbonylacetylacetonate by Fayer and coworkers.[6]

4 ISOTOPOLOGUE SIGNALS

Table S2. Computed vibrational energy shifts of the relevant ^{13}C isotopologues of the chelate **1-spc**-κ^2O,O'·$Mg^{2+}(MeCN)_4$ relative to the all-^{12}C compound in MeCN (M06/6−31+G(*d*,*p*)/PCM/Bondi).

	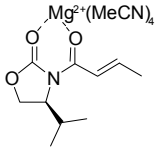	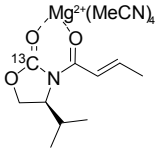	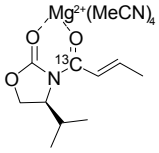	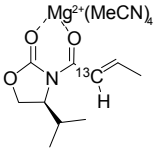	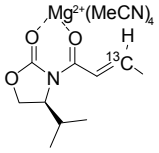
	(cm^{-1})	Δ (cm^{-1})	Δ (cm^{-1})	Δ (cm^{-1})	Δ (cm^{-1})
ν_1	1666	–3	–31	–14	–15
ν_2	1707	–9	–6	–12	–15
ν_3	1810	–36	–6	–1	–1

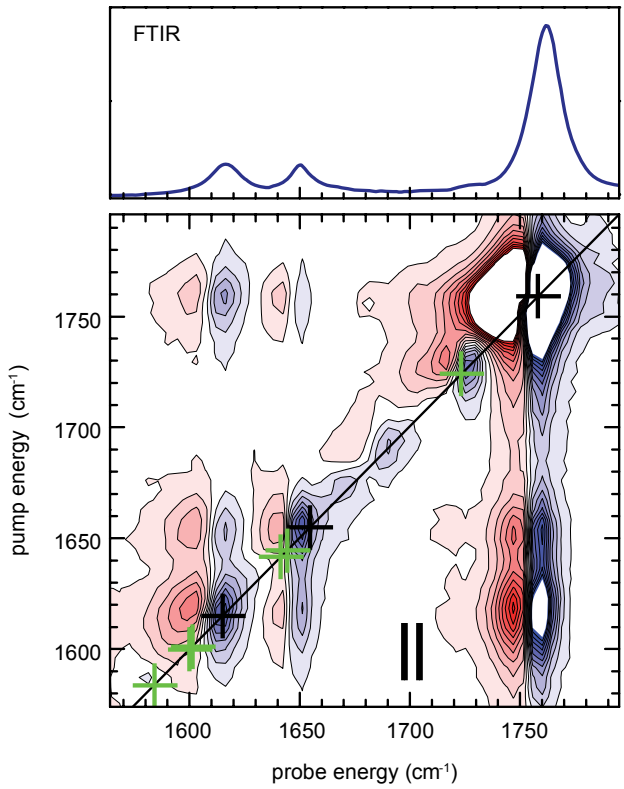

Figure S6. Computed positions (green crosses) for the diagonal peaks of the ^{13}C isotopologues of the major species **1-spc**-κ^2O,O'·$Mg^{2+}(MeCN)_4$ in the P2D-IR spectrum of the mixture of **1** and $Mg(ClO_4)_2$ in MeCN. The computed vibrational energies are corrected by –51 cm^{-1}. Only the peaks with shifts larger than 10 cm^{-1} compared to the all ^{12}C isotopologue (black crosses) are shown.

5 REFERENCES

(1) Frisch, M. J.; Trucks, G. W.; Cheeseman, J. R.; Scalmani, G.; Caricato, M.; Hratchian, H. P.; Li, X.; Barone, V.; Bloino, J.; Zheng, G.; Vreven, T.; Montgomery, J. A.; Petersson, G. A.; Scuseria, G. E.; Schlegel, H. B.; Nakatsuji, H.; Izmaylov, A. F.; Martin, R. L.; Sonnenberg, J. L.; Peralta, J. E.; Heyd, J. J.; Brothers, E.; Ogliaro, F.; Bearpark, M.; Robb, M. A.; Mennucci, B.; Kudin, K. N.; Staroverov, V. N.; Kobayashi, R.; Normand, J.; Rendell, A.; Gomperts, R.; Zakrzewski, V. G.; Hada, M.; Ehara, M.; Toyota, K.; Fukuda, R.; Hasegawa, J.; Ishida, M.; Nakajima, T.; Honda, Y.; Kitao, O.; Nakai, H.; Vreven, T.; Montgomery, Jr., J. A.; Peralta, J. E.; Ogliaro, F.; Bearpark, M.; Heyd, J. J.; Brothers, E.; Kudin, K. N.; Staroverov, V. N.; Kobayashi, R.; Normand, J.; Raghavachari, K.; Rendell, A.; Burant, J. C.; Iyengar, S. S.; Tomasi, J.; Cossi, M.; Rega, N.; Millam, J. M.; Klene, M.; Knox, J. E.; Cross, J. B.; Bakken, V.; Adamo, C.; Jaramillo, J.; Gomperts, R.; Stratmann, R. E.; Yazyev, O.; Austin, A. J.; Cammi, R.; Pomelli, C.; Ochterski, J. W.; Martin, R. L.; Morokuma, K.; Zakrzewski, V. G.; Voth, G. A.; Salvador, P.; Dannenberg, J. J.; Dapprich, S.; Daniels, A. D.; Farkas, Ö.; Foresman, J. B.; Ortiz, J. V.; Cioslowski, J.; Fox, D. J. *Gaussian 09 Revision B.01*; Gaussian Inc. Wallingford CT, 2009.

(2) Zhao, Y.; Truhlar, D. G. *Theor. Chem. Account* **2008**, *120*, 215–241.

(3) Messmer, A. T.; Lippert, K. M.; Steinwand, S.; Lerch, E.-B. W.; Hof, K.; Ley, D.; Gerbig, D.; Hausmann, H.; Schreiner, P. R.; Bredenbeck, J. *Chem. Eur. J.* **2012**, DOI: 10.1002/chem.201201583.

(4) Tomasi, J.; Mennucci, B.; Cammi, R. *Chem. Rev.* **2005**, *105*, 2999–3094.

(5) Bondi, A. *J. Phys. Chem.* **1964**, *68*, 441–451.

(6) Rector, K. D.; Kwok, A. S.; Ferrante, C.; Tokmakoff, A.; Rella, C. W.; Fayer, M. D. *J. Chem. Phys.* **1997**, *106*, 10027.